ORIGINAL ARTICLE

CFRP-strengthened RC beams under fire condition: numerical model

Vigas de concreto armado reforçadas com CFRP em situação de incêndio: modelo numérico

Thiago Brazeiro Carlos[a] ID
Valdir Pignatta e Silva[a] ID

[a]Universidade de São Paulo – USP, Escola Politécnica, Departamento de Engenharia de Estruturas e Geotécnica, São Paulo, SP, Brasil

Abstract: The Carbon Fiber Reinforced Polymer (CFRP) has excellent flexural performance on strengthening and rehabilitation of reinforced concrete (RC) structures. However, it is known that CFRP strengthening systems are very vulnerable to high thermal exposure. To provide a better understanding of its fire behavior and fulfill gaps in this field, this investigation proposes the development of an accurate three-dimensional (3D) Finite Element (FE) model capable of simulating the CFRP-strengthened RC beams flexural behavior at ambient temperature and under fire conditions. To achieve the goals, thermal and mechanical numerical simulations have been performed to validate the developed FE models. Experimental results reported in two parallel studies were used to model's validation. The numerical model has been satisfactorily validated and the results had a good predictability with the experimental results in terms of thermal and mechanical behavior.

Keywords: fire, reinforced concrete structures, beam, CFRP strengthening, numerical model.

Resumo: Os Polímeros Reforçados com Fibras de Carbono (CFRP) possuem excelente desempenho à flexão no reforço e reabilitação de estruturas de concreto armado. No entanto, sabe-se que os sistemas de reforço de CFRP são muito vulneráveis à alta exposição térmica. Para fornecer uma melhor compreensão do seu comportamento em incêndio e preencher lacunas da área, o estudo propõe o desenvolvimento de um modelo tridimensional de elementos finitos consistente, capaz de simular o comportamento à flexão de vigas de concreto armado, reforçadas com CFRP, sob condições de temperatura ambiente e de incêndio. Para atingir os objetivos, simulações numéricas, térmicas e mecânicas, foram realizadas para validar os modelos desenvolvidos. Resultados experimentais relatados em dois estudos paralelos foram utilizados para a validação do modelo. O modelo numérico foi satisfatoriamente validado e os resultados tiveram uma boa previsibilidade aos resultados experimentais, em termos de comportamento térmico e mecânico.

Palavras-chave: incêndio, estruturas de concreto armado, viga, reforço, CFRP, modelo numérico.

1 INTRODUCTION

The temperature variation significantly affects the mechanical performance of the CFRP strengthening system on concrete structures. Thus, the knowledge of the temperature effects is a key factor in the fire design of this type of construction, especially as it develops at the CFRP-concrete bond which is a critical zone very sensitive to thermal exposure.

The failure of bond generally occurs at temperatures near or above the Glass Transition Temperature (T_g)[1] of the adhesive. Glass Transition Temperature is the point at which a material alters state – going from a glass-like rigid solid to a more flexible compound. T_g is normally measured on a Differential Scanning Calorimeter (DSC) piece equipment. However, in some cases, the bond failure happens for temperatures below T_g. The T_g of the adhesive varies usually from 50 and 120 ºC [1]–[5], depending on the polymeric matrix of constituents and the type of resin, among others. The better understanding of the temperature effects on this type of structures makes it possible for reliable and safe design in case of fire. To contribute to this end, few numerical investigations concerning the fire behavior of CFRP-strengthened RC members have been carried out over the last years [6]–[10], as discussed in detail in the next section.

2 STATE OF THE ART

As mentioned in the previous section, recent concerns about the fire influence on CFRP-strengthened RC beams structures have generated few numerical investigations in this area, to better understand their behavior at elevated temperatures. Relevant numerical studies on fire behavior of CFRP-strengthened RC beams structures [6]–[10] are presented in detail below.

Hawileh et al. [6] numerically investigated the fire behavior of thermally insulated EBR-CFRP-strengthened T-section RC beams previously fire-tested by Williams et al. [11] which was described in the previous section. For this purpose, detailed 3D FE models were developed using the commercial software ANSYS [12] to perform a nonlinear transient thermal-stress analysis under fire conditions. The FE models were composed by thermal and structural elements, to enable independent thermal and structural analysis. The temperature-dependence of thermal and mechanical properties of the constituent materials of the specimens were considered, including CFRP and passive fire protection materials. Numerical results were compared with experimental data [11] in terms of temperature evolution in the beam, in the CFRP, in the reinforcements, along the CFRP-concrete interface as well as the deflections of the beams when subjected to fire. The heating was applied only at the bottom surface of the specimens in a transient state according to ASTM E119 [13]. In addition, a sustained uniformly distributed load at the top surface of the T-beam was applied to simulate the serviceability loads during heating. The numerical models presented a good predictability with the experimental results in terms of temperatures. Regarding the predicted mid-span vertical deflections as a function of fire exposure time, the results also showed a good agreement with the ones experimentally measured in the first 33 minutes of test (until the hydraulic pressure was lost accidentally in the experiment). However, the authors were unable to validate the numerical procedure in terms of mechanical response (such as the CFRP debonding phenomenon) due to limited experimental data.

Ahmed and Kodur [7] improved a numerical approach previously developed by Kodur and Ahmed [14] regarding the modelling of the degradation of connections of reinforced RC beams with EBR-CFRP laminates exposed to fire. The main innovation presented by [7] was the simulation of the bond degradation at the CFRP-concrete interface by means of an explicit model by means of the bond-slip laws, which was not considered in the previous study [14]. The numerical procedure was implemented into a macroscopic FE model which is capable of predicting the temperature-dependency of material properties, different fire scenarios, and failure limit states in evaluating fire response of CFRP-strengthened RC beams. The numerical model validity and accuracy was based on the experimental data from fire resistance tests on CFRP-strengthened RC beams performed by Blontrock et al. [15] and Ahmed and Kodur [16]. Moreover, a parametric study has been carried out on another CFRP-strengthened RC beam [17] to simulate the effect of bond degradation and insulation schemes at CFRP–concrete interface response under fire situation. Overall, according to the results a good agreement between the experimental and numerical FE models was obtained in terms of temperatures, as well as the deflections and the instant to CFRP debonding. Regarding to parametric analysis, the results showed a significant bond degradation in moment capacity and stiffness when the temperature at CFRP–concrete interface slightly exceeds T_g of the adhesive (81 ºC), leading to the initiation of CFRP laminate debonding (around 40 min of fire exposure). In addition, the authors concluded that the time the bond degradation in CFRP-strengthened concrete members occurs depends on the fire protection thickness and T_g of the adhesive.

Dai et al. [8] developed the first 3D FE model for the simulation of the thermomechanical behavior of insulated EBR-CFRP-strengthened RC beams under fire conditions. The 3D FE models were developed and validated based on the experimental data and results from fire resistance tests performed by Blontrock et al. [15] and Williams et al. [11], both described in the previous section through the commercial software package Abaqus [18]. The bond degradation with temperature evolution for the internal steel reinforcement, the external CFRP, the temperature-dependence of thermo-physical and mechanical properties of all materials were considered in the simulations. The bond-slip laws recommended in Model Code [19] for ambient temperature were used to represent the interaction between the concrete surface and steel reinforcements. The proposed numerical approach achieved a good accuracy of thermal and structural

response of thermally protected EBR-CFRP strengthened RC beams under fire conditions in comparison to the ones obtained in experimental studies (Blontrock et al. [15] and Williams et al. [11]). Numerical results show that the consideration of a perfect bonding between CFRP and concrete leads to underestimations of fire resistance in CFRP-strengthened RC beams, as adopted in most of previous numerical investigations.

Another relevant numerical investigation on the fire behavior of RC beams strengthened with CFRP laminates bonded according to EBR technique was performed by Firmo et al. [9]. Two-dimensional FE models were developed to simulate fire resistance tests of simply supported RC beams strengthened with EBR-CFRP laminates previously studied by Firmo and Correia [20] (described in detail in previous section) and Firmo et al. [21]. The thermomechanical response of models was numerically simulated considering the influence of CFRP anchorage systems and different passive fire protection schemes applied along the bottom surface of the beams and in the anchorage zones. The commercial software package Abaqus [22] was used in the numerical simulations where the temperature variation of the thermomechanical properties of the materials was considered and the CFRP-concrete bond interaction was modelled based on bi-linear bond-slip laws previously calibrated for different temperatures (up to 120 ºC). The numerical results showed a good accuracy in terms of fire behavior of CFRP-strengthened RC beams, including the "cable mechanism" phenomena, the time and temperature at debonding of the strengthening system as observed in the reported experimental results [20], [21]. Furthermore, this numerical study allowed the validation of the proposed bond-slip laws for the CFRP-concrete bond interaction, showing their suitability for simulating the behavior of EBR-CFRP-strengthened RC beams subjected to fire.

A more recent and detailed numerical investigation carried out by Firmo et al. [10] (improving their initial study mentioned above [9]) proposed 3D FE models to simulate the fire response of the RC beams strengthened with CFRP laminates bonded according to the EBR technique. The CFRP-concrete bond interaction was modelled by bi-linear bond-slip laws as well as the one previously validated by Firmo et al. [9] with Abaqus [22] software. According to results, the structural response of the CFRP-strengthened RC beams was achieved with reasonable accuracy when compared with experimental results obtained in fire resistance tests [20], despite some deviations observed. These satisfactory results confirmed that the bond-slip laws for the CFRP-concrete interaction, previously used in the 2D FE model by Firmo et al. [9], can be used for the 3D simulation of EBR-CFRP strengthening systems subjected to fire conditions and allow more complex analyses. Moreover, the possibility of exploring the mechanical contribution of the CFRP in a fire situation by a "cable" behavior with the application of a thicker insulation in the CFRP anchorage zones is highlighted.

The literature review described above shows that the numerical efforts to simulate the fire behavior of CFRP-strengthened concrete beams are very limited. Few numerical studies have considered the CFRP-concrete interface's thermal degradation and have used 3D models that are theoretically more realistic. Moreover, numerical results have shown that accurate predictions of the fire response of CFRP-strengthened beams require the inclusion of explicit temperature-dependent bond-slip models for the CFRP-concrete interface, which has been neglected in most of the above-cited studies.

In addition to numerical studies on fire behavior of CFRP-strengthened beams, a few analytical and numerical investigations reported in the literature [23]–[28] have focused specially on the behavior of the bond between the CFRP and concrete at elevated temperatures in strengthening systems. However, some gaps in this field were also noted. Most of these studies were limited to the T_g of the adhesive. Moreover, simplifications assumed by the authors on the bond-slip relationships for higher temperatures, such as the consideration that the concrete-adhesive interface is linear elastic, did not provide good results for temperatures above or much higher than T_g (although good accuracy has been observed for temperatures below T_g).

3 JUSTIFICATION AND OBJECTIVES

In the past, the development of research allowed the elaboration and implementation of standards for ambient temperature design of concrete structures that resulted in the elaboration of EN 1992-1-1 [29]. However, for fire design of CFRP-strengthened concrete elements, there is still a lack of research. Currently, the methods presented in EN 1992-1-2 [30] for fire design of concrete structures do not consider the contribution of the CFRP strengthening on the flexural behavior of these elements under fire conditions and do not have consistent methods for fire design. Furthermore, there are other important standards for specific design of externally bonded FRP systems for strengthening existing structures, such as ACI 440.2R-17 [5] and Fib bulletin 14 [31]. Both recognize the inefficiency of CFRP strengthening systems at elevated temperatures, but they do not define any calculation criteria or method that consider the contribution of the CFRP in the case of fire. The ACI and Fib documents [5], [31] are overly conservative when they simply suggest that the fire verification of the structure may be conducted considering that the strengthening is

non-existent, i.e., that the contribution of the resistance of the CFRP system to the service conditions verifications is not considered. Therefore, the development of new design methods for concrete structures strengthened with CFRP subjected to fire are urgently and necessary given the substantial current demand for their use in buildings and due to the inherent risks of a composite structural element when subjected to these limit conditions. This research intends to contribute to this purpose.

Despite the investigations carried out over the years (as discussed in Chapter 2), many issues concerning the bond behavior between concrete and CFRP strengthening systems at elevated temperatures remain unclear and need further investigation, especially concerning the limited temperature ranges studied. Thus, the thermal and mechanical response of the CFRP-concrete bond for temperatures higher and much higher than T_g needs further investigation.

Based on the challenges discussed above, it is fundamental the development of accurate models to simulate the CFRP-concrete bond behavior with good predictions for temperatures above T_g and that consider the complexities mentioned above are essential. In this regard, the present research intends to be an important contribution in fire safety engineering, since its objective is the develop an accurate model capable to simulate the fire behavior of CFRP-strengthened concrete beams, based on valuable experimental results reported in two parallel studies by Carlos et al. [32] and by Carlos and Rodrigues [33]. Therefore, this research becomes essential to bring a deep/better understanding and fill the gaps on the fire behavior of this type of composite structures, also contributing to further research. Moreover, the development of the FE model can be used in parametric studies, to assess different parameters not experimentally tested yet and contribute to the advancement of the area.

4 NUMERICAL INVESTIGATION

4.1 Model geometry

The FE models' geometry consisted of a replication of the ones that composes the beams tested in the experimental investigation by Carlos et al. [32] (Figure 1a), as well as for the other elements and materials involved. Three-dimensional FE models of simply supported RC beams flexurally strengthened with EBR-CFRP laminates (Figure 1b) were modelled using the commercial software package Abaqus to simulate the mechanical response at ambient and elevated temperatures. In addition, 3D models of unstrengthened beams were also developed for the mechanical analysis.
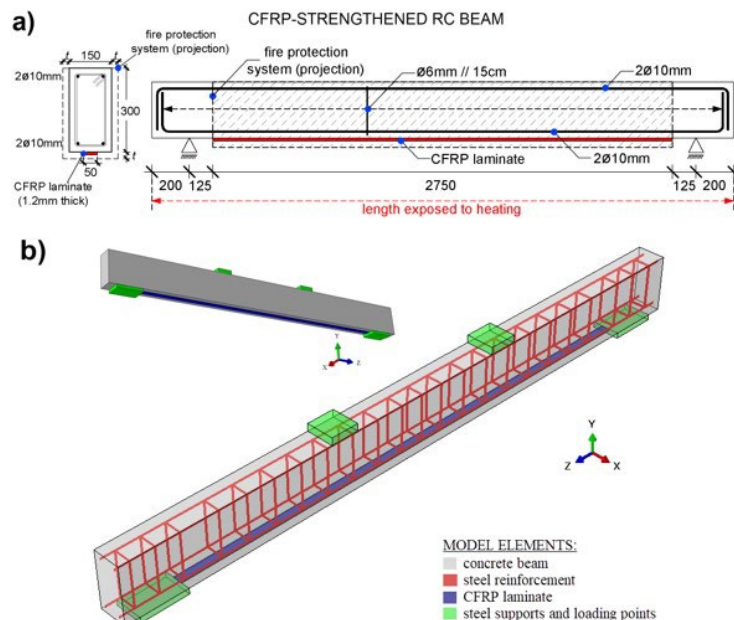

Figure 1. a) Geometry of the beams tested in the experimental investigation by Carlos et al. [32] and b) representative 3D numerical model of the CFRP-strengthened beam for mechanical analysis at ambient and elevated temperatures (not to scale, dimensions in mm).

Two-dimensional (2D) FE models for both type of beams were also developed exclusively for the heat transfer analysis since this is a type of uncoupled analysis. The 2D models were developed based on the tested cross-sections of the beams, including the modelling of the concrete slab cross-section to simulate the thermal interactions between the elements, as intended in the experimental study [32]. The use of three different fire protection materials, the ones previously fire tested in the CFRP-strengthened beams by Carlos et al. [32], were also numerically investigated in terms of thermal response.

The CFRP-strengthened RC beams were protected by three types of fire protection systems composed of the following sprayed materials: Vermiculite-Perlite (VP), ordinary Portland cement with Expanded Clay aggregates (EC) and Ordinary Portland (OP) cement-based mortars. These materials are described in further detail in section 4.3.1.4.

Four representative heat transfer models (Figure 2a-d) were numerically simulated under fire conditions. The nomenclature adopted for the 2D FE models of the beams is analogous to the ones experimentally tested specimens [32]. The unstrengthened and unprotected RC beam is referred to by RC. The predicted results of these simulations were compared with the experimental data obtained by Carlos et al. [32] in terms of temperatures vs. time of fire exposure at different locations of the mid-span cross-section. To allow comparison between results, the same thermocouples arrangement used in the previous experimental study [32] was defined in the current heat transfer analysis, as shown in Figure 3a and Figure 3b for the unstrengthened and CFRP-strengthened beams, respectively.
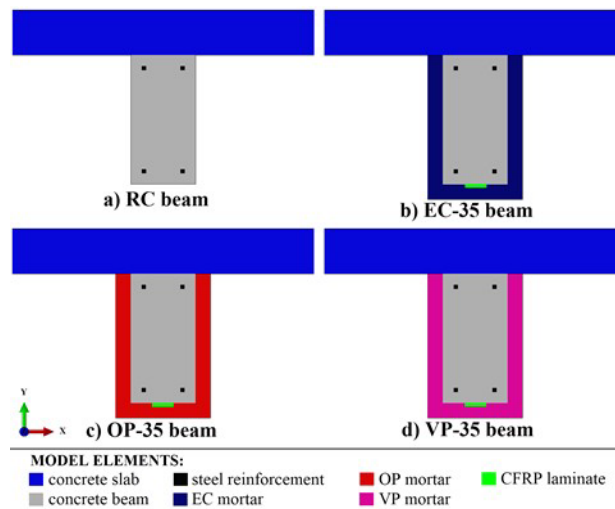

Figure 2. Numerical models for heat transfer analysis: (a) RC beam, (b) EC-35 beam, (c) OP-35 beam and (d) VP-35 beam (not to scale).
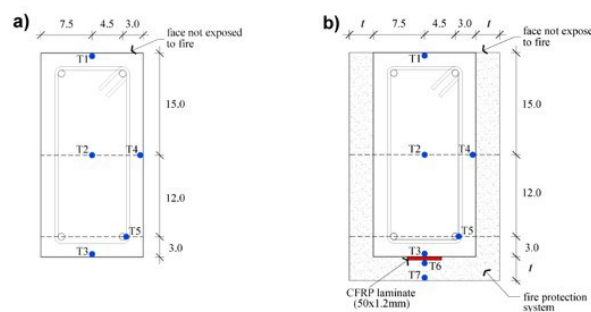

Figure 3. Location and nomenclature of thermocouples at Section S1 of (a) unstrengthened and (b) CFRP-strengthened RC beams (not declared units in cm).

4.2 Finite Element Type

The RC beams were modelled by using solid elements (C3D8R) for the concrete material geometry, steel supports and loading points. The C3D8R finite element was also chosen for modelling the CFRP laminate in the case of

strengthened RC beams. The longitudinal steel reinforcement and stirrups were modelled by using truss elements (T3D2).

The C3D8R element (Figure 4) is defined as a three-dimensional, continuum (C), hexahedral and an eight-node brick element with reduced integration (R), hourglass control and first-order (linear) interpolation. These finite elements have three degrees of freedom per node, referring to translations in the three directions X, Y and Z (global coordinates). One of the reasons for using the C3D8R in the current research is because it can be applied in Abaqus for linear analysis and complex nonlinear analyses involving contact, plasticity, and large deformations. Moreover, they are available for stress, heat transfer, acoustic, coupled thermal-stress, coupled pore fluid-stress, piezoelectric, and coupled thermal-electrical analyses [34].
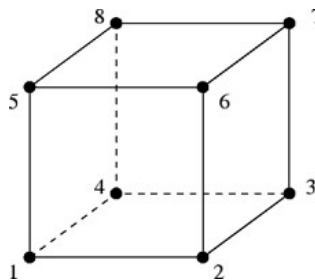
Figure 4. Scheme of the C3D8R element [34]

The selected C3D8R element type uses a reduced (lower-order) integration to form the element stiffness with only one integration location per element. The reduced integration method was chosen because it reduces the amount of CPU time necessary for analysis of the model and avoids shear locking without losing the accuracy of the analysis. Shear locking may occur in elements under pure bending and without reduced integration, because the element edges must remain straight and the angle between the deformed isoparametric lines is not equal to 90º which means that the strain in the thickness direction is not zero (Figure 5). So, this can lead to overestimation of the load capacity in bending dominated problems [35].
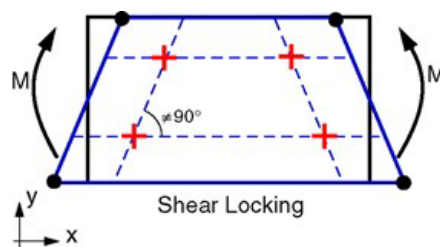
Figure 5. Shear locking in elements without reduced integration points [34]

T3D2 is a three-dimensional and two-node element used to model slender, line-like structures that support loading along the axis only or the centreline of the element (Figure 6). No moments or forces which are perpendicular to the centreline are supported. This element allows defining the cross-sectional area associated with the truss element as part of the section definition. When truss elements are used in large-displacement analysis, the updated cross-sectional area is calculated by assuming that the truss is made of an incompressible material, regardless of the definition of the material being analysed. This assumption is adopted because the most common applications of trusses at large strains involve yielding metal behaviour or rubber elasticity, in which cases the material is effectively incompressible [34].
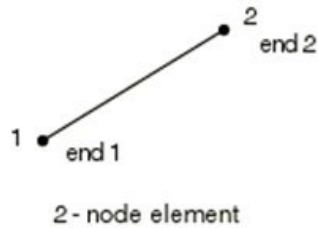
Rev. IBRACON Estrut. Mater., vol. 16, no. 2, e16202, 2023

6/18

Figure 6. Scheme of the T3D2 element [34]

For the 2D heat transfer analysis, the DC2D4 element was selected. This element type consists of a 4-node linear heat transfer quadrilateral element and was chosen because it presents excellent accuracy to estimate the temperature evolution of different materials in a thermal analysis.

Additional information about the aforementioned finite elements can be seen in detail in [36].

4.3 Material modelling

The properties of the materials used in the FE models were represented in the Abaqus program based on the literature and standardization. So, it was intended to reproduce the thermophysical and mechanical behavior of the tested beams as faithfully as possible, as described in detail in the following sections.

4.3.1 Thermophysical material properties

4.3.1.1 Concrete

In the modelling of the specific heat for concrete (c_p), a higher value of 8.5% for the moisture content was defined according to the humidity conditions of the concrete specimens. Therefore, the $c_{p.peak}$ for the moisture content of 8.5% corresponded to 4040 J/kgºC. This specific heat peak is because the evaporation of the free water from the concrete occurs through endothermic reactions. The evolution of the specific heat value in relation to the temperature adopted for the concrete used in the current investigation was based on the recommendations of Eurocode 2, part 1-2 [30]. The thermal conductivity of ordinary concrete for a given temperature was proposed based on the expressions provided in the National French Annex to NF EN 1992-1-2 [37]. Therefore, the curve established by the French Annex [37] was selected to be applied to the developed model. In the current model, the usual density of the single concrete at 20ºC [ρ (20 ºC)] was defined as 2300 kg/m³, as suggested in Eurocode 2, part 1-2 [30]. The emissivity of the concrete surface was defined as 0.7 and it was considered constant with temperature evolution, according to Eurocode 2, part 1-2 [30]. The radiative heat flux was calculated using the emissivity coefficients of the electric resistance of the furnace and of the concrete surface, both equal to 0.7, and it resulted in a value of 0.49. A convection coefficient of 15 W/m² ºC (also constant with temperature) was adopted as suggested in EN-1992-1-2 [30].

4.3.1.2 Steel reinforcement

In the case of steel reinforcement modelling, the thermophysical material properties were defined based on Eurocode 4, part 1-2 [38] recommendations. The specific heat of steel reinforcement (c_s) at different temperatures in the numerical model was determined by the curve defined in EN 1994-1-2 [38]. The thermal conductivity of the steel was also defined according to EN 1994-1-2 [38]. According to Eurocode 4, part 1-2 [38], the steel reinforcement density (ρ_s) was defined constant with temperature, corresponding to 7850 kg/m³.

4.3.1.3 CFRP laminate

The CFRP laminates were thermally characterized in the numerical model using experimental data from the literature [39], [40]. The variation of the specific heat of CFRP laminates was modelled based on experimental data reported in the investigation by Griffis et al. [39]. Similarly to the specific heat variation, the proposal presented in Griffis et al. [39] for the evolution of the CFRP thermal conductivity in relation to temperature was adopted. The density of the CFRP was determined based on the relationship of the remaining mass with temperature according to results obtained by Thermogravimetric Analysis (TGA) performed by Firmo et al. [40]. Thus, considering the mass loss

relationship determined in [40] and a density of 1550 kg/m³ at ambient temperature according to the manufacturer [41], the variation of the density in relation to temperature was defined.

4.3.1.4 Fire protection systems

The VP mortar was a commercial mortar made with lightweight expanded perlite and vermiculite aggregates, refractory compounds, cementitious binders, and a ratio water/compounds of 0.67–0.80 l/kg. Also, this fire protection material presents a dry density of 450–500 kg/m3 and a thermal conductivity of 0.0581 W/m·K [42]. The OP mortar, also commercial, was formulated from hydraulic binders, calcareous, siliceous aggregates, and some other non-specified additions, with dry density of 1500–1800 kg/m3, thermal conductivity 0.67 W/m·K and a ratio water/compounds of 0.13–0.15 l/kg [43]. The EC mortar differed from the OP mortar by replacing the calcareous aggregates by expanded clay aggregates. A ratio water/compounds of 0.35–0.40 l/kg was used. The expanded clay is a lightweight aggregate with a granulometry distribution of 0.25–2.0 mm, a dry density of 468–633 kg/m3 and a thermal conductivity of 0.13 W/m·K [44]. This material was incorporated into the mortar mixture in a ratio of 2.6:1 (cement:aggregate). The aforementioned thermal property values are for ambient temperature.

4.3.2 Mechanical material properties

4.3.2.1 Concrete

The mechanical properties of the concrete at ambient temperature were experimentally determined and given in EN 1992-1-1 [29]. Thus, an average cube compressive strength of f_{cm}=30.1 MPa was experimentally obtained in this work by means of compressive strength tests. The average tensile strength (f_{ctm}) was defined as 2.9 MPa according to [29]. Concerning the modulus of elasticity of concrete (E_{cm}), it was calculated for thermal actions (natural fire simulation) in accordance with a mathematical model for stress-strain relationships of concrete under compression at elevated temperatures proposed in EN 1992-1-2 [29]. The E_{cm} was calculated as 17.3 GPa (this value is generally lower than the one defined for concrete at ambient temperature). The reduction of the mechanical properties of the concrete at elevated temperatures were obtained from the relationships suggested in EN-1992-1-2 [30] and EN 1994-1-2 [38]. The Poisson's ratio was defined equal to 0.2 and constant with temperature, according to Eurocode 2, part 1-1 [29] recommendation.

4.3.2.2 Steel reinforcement

The mechanical properties of the steel reinforcement (B500 steel class) were defined according to Eurocode 4, part 1-2 [38]. The mechanical properties of the steel rebars at ambient temperature were as follows: yield stress of 500 MPa, modulus of elasticity of 210 GPa, ultimate tensile strength of 550 MPa and Poisson's ratio (v) of 0.3. The temperature-dependent behavior of steel was also determined by part 1-2 of Eurocode 4 [38], following the reduction factor proposals presented in this standard. Poisson's ratio was considered constant with temperature. The strain hardening effect on the steel at elevated temperatures was also accounted for in current numerical investigation and was calculated based on the calculation methods proposed by the part 1-2 of Eurocode 4 [38] (allowed by the stress-strain relationships for steel at elevated temperatures).

4.3.2.3 CFRP laminate

Regarding the mechanical behavior of the CFRP laminates, they behave essentially in the longitudinal direction in the present application, hence, as a simplification, the CFRP was modelled as linear elastic isotropic. The temperature influence on mechanical behavior of CFRP laminate in the current model was based on the relations proposed by Wang et al. [45] and Bisby [46] for the tensile strength and modulus of elasticity, respectively. The laminates have an average tensile strength of 2800 MPa, modulus of elasticity of 170 GPa and ultimate strain of 16.0‰ at ambient temperature, according to the manufacturer [41]. The Poisson's ratio is 0.3 (constant with temperature).

4.3.2.4 Fire protection systems

Concerning the fire protection systems, their mechanical contribution was not considered since it is expected to be negligible.

4.4 Finite element mesh

The finite element size significantly influences the behavior of the CFRP-strengthened RC beams. In an analysis based on the finite element method, the accuracy of the results is closely related to two aspects: first, the use of appropriate elements for each type of analyses, based on the structure geometry or material, interpolation degree and integration scheme; second, the correct model discretization defined from a sensitivity study, where a comparison of meshes with different arrangements or densities must be performed.

In the current research, three different mesh densities were studied to verify the effect of the finite element size on the behavior of the unstrengthened and CFRP-strengthened RC beams. The meshes were defined (for both type of beams) based on a relatively coarse, intermediate, and finer refinement level, corresponding to the densities (for the largest element) of 35 x 35 mm, 25 x 25 mm, and 15 x 15 mm.

The mesh study on CFRP-strengthened beams presented a high similarity between the different densities.

Finally, an excellent similarity and simulation stability between the predicted load vs. displacement evolution was obtained by using finite element meshes of 15 x 15 mm and 25 x 25 mm for both types of beams. To save computational time, finite element meshes of 25 x 25 mm were adopted in all models simulated in this research, as presented in Figure 7.
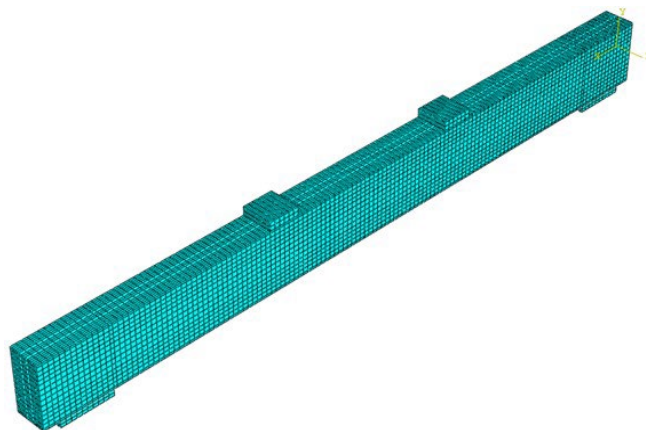

Figure 7. Finite element meshes studied for the CFRP-strengthened and unstrengthened RC beam with maximum densities of 25 mm

4.5 Boundary, loading and contact conditions

To reproduce the real test set-up as reported by Carlos et al. [32], the supports of the beam and the loading were also modelled in the numerical models on rigid plates attached to the beams to distribute possible concentrated forces on them. This representation on a numerical model is shown in Figure 8. The models were subjected to a fixed mechanical load applied to the direction -Y in a four-point bending configuration (see Figure 8) as used in the experimental tests [32]. The preload applied in the simulations (24 kN) correspond to 70% of the design value of the loadbearing capacity of the RC beam at ambient temperature, as defined in the experimental test procedure [32]. Regarding the support system, all degrees of freedom of the nodes located on the bottom surface and at the middle of the respective rigid plate were constrained to simulate the pinned support, whereas for the roller support only the translations in the directions X and Y were constrained. In addition, all nodes located at each end of both supports were constrained to translations in the direction X to prevent their lateral deformation (Figure 8).
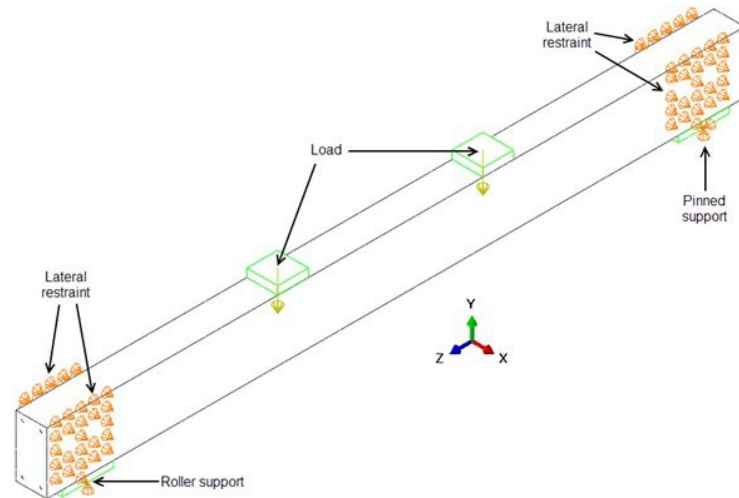
Figure 8. Boundary and loading conditions of 3D numerical models used in the FE analysis.

Concerning the contact conditions, the surface-to-surface contact method was used to simulate the contact between the concrete beam and the other materials. Small-sliding formulation was used in the contact tracking algorithm between the beams and the CFRP laminates. In this case, the geometric nonlinearity is included in the model. A penalty method (damage) was defined as the cohesive contact property between the concrete and CFRP surfaces. Thus, two bond damage criteria were adopted: maximum nominal stress and fracture energy. These values (temperature-dependent) were inputted in the FE model based on the experimental data obtained from the SST tests performed by Carlos and Rodrigues [33].

Finally, the fire action was applied in the 3D model. The heat transfer step was applied after the preloading of the model and performed according to the furnace temperatures registered in the experimental tests to validate the FE model. In these simulations, a 4-node linear heat transfer quadrilateral element (DC2D4) was chosen and a 2D numerical model was developed to estimate the temperature distribution in the cross-sections of the beams. To accurately simulate the experimental test conditions [32], the bottom and lateral surface of the models of the beams were directly exposed to the heating. The upper face of the beam in the model was superposed by a surrounding concrete slab which in turn was submitted to a constant ambient temperature, as adopted in the experimental tests [32]. The initial temperatures of the models were defined based on the measurements recorded in the experimental tests [32]. Radiation and convection heat transfer modes were considered on exposed surfaces. The resultant emissivity was taken as 0.49, considering the emissivity coefficients of the electric resistance of the furnace and the beams both equal to 0.7. A convection coefficient of 15 W/m^2 °C (constant with temperature) was adopted, as suggested in EN-1992-1-2 [30].

A constant and uniform temperature corresponding to ambient temperature was defined at beam supports and at loading application points, since these elements were fire-protected.

4.6 Analysis method and procedure

Geometrical and material non-linear analysis were employed in the developed FE model. The non-linear equations were solved iteratively using the Newton Raphson's Method. The main advantage of Newton's method is its quadratic convergence rate when the approximation at iteration is within the "radius of convergence", i.e., when the gradients defined by matrix provide an improvement to the solution. The method disadvantage is because the Jacobian matrix must be calculated, and this same matrix must be solved. The solution of the Jacobian matrix can be a problem due to the computational effort involved. The direct solution to linear equations can dominate the entire computational effort, as the complexity of the problem increases. Despite the high computational effort required, Moltubakk [47] states that this method needs few iterations to reach the convergence capable of establishing the final solution.

The prediction of the non-linear concrete behavior was defined considering a plastic damage model: Concrete Damaged Plasticity.

The plastic damage model is the most used model since it has greater convergence capacity compared to the average crack model due to the greater simplicity and robustness of the associated numerical algorithms, which makes the use of this model more attractive in the analysis of more complex structures [48].

The Concrete Damaged Plasticity assumes two mechanisms of concrete failure, tensile cracking and compression crushing. Crack propagation is modeled based on a continuous damage mechanism: Stiffness Degradation.

A sequentially uncoupled thermo-mechanical analysis was adopted to simulate the fire behaviour of the CFRP-strengthened RC beams. A heat transfer analysis was first performed to obtain the temperature distributions along the cross-section of the beam by 2D FE models, followed by a 3D mechanical analysis that considered the thermal data influence provided in the previous step. Therefore, in the Abaqus software the thermo-mechanical response of the specimens (allowed after the uncoupled analysis) was simulated by a two-step analysis. In the first step, the desired loading was applied under displacement control to the FE model at ambient temperature and it was fixed afterwards, inducing an initial deflection (as occurred in the reference experimental model [32]). The loading step was explicitly defined in the Abaqus. In the second step, the temperature distributions in relation to time (previously determined in the thermal analysis) were imposed to the loaded beams for a duration like that observed in the reference fire resistance tests [32]. In the case of validation of models at ambient temperature, only a structural analysis was performed with the purpose of simulating the behavior of unstrengthened and CFRP-strengthened RC beams up to failure.

5 RESULTS AND DISCUSSIONS

5.1 Mechanical response at ambient temperature

Numerical simulations on an unstrengthened and EBR-CFRP-strengthened beam (referred as RC_AT and CFRP_AT, respectively) were performed to assess the ability and accuracy of the 3D FE models described above in predicting the mechanical response of these beams. The results of experimental tests reported in a relevant parallel study by Carlos et al. [32] were used for FE model's validation. Figure 9 shows a comparison of the load vs. vertical mid-span displacement curves for the unstrengthened and CFRP-strengthened RC beams obtained from the experimental tests (Exp.) [32] and FEA (Num.).
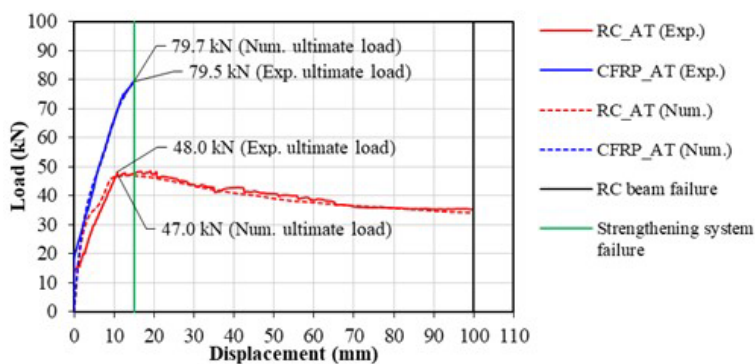

Figure 9. Experimental (Exp.) [32] and predicted (Num.) load vs. mid-span displacement curves for the unstrengthened and CFRP-strengthened RC beams at ambient temperature.

Figure 9 reveals that all predicted results generally fit closely with the experimental curves for both specimens, especially for obtained peak loads (ultimate load). The ultimate predicted load of the RC_AT and CFRP_AT beams was 47.0 kN and 79.7 kN, respectively. The ultimate load experimentally obtained for the unstrengthened and CFRP-strengthened beams was 48.0 and 79.5, respectively. These results were very similar to those obtained numerically for both specimens. Therefore, the values of the predicted-to-experimental loading capacity ratios (P_{NUM} / P_{EXP}) for the RC_AT and CFRP_AT beams correspond to 0.98 and 1.00, respectively. Finally, an excellent agreement and accuracy between the experimental and numerical results was noticed, ensuring a strong validity of the developed FE model in predicting the mechanical response of both RC beams strengthened with EBR-CFRP laminate and unstrengthened RC beam at ambient temperature.

5.2 Mechanical response under fire conditions

The experimental results from fire resistance tests carried out by Carlos et al. [32] on the CFRP-strengthened beam EC-35 were used to validate the mechanical response of the 3D numerical model under fire conditions (see Figure 10b). Furthermore, for the mechanical validation of the FE model that represents the RC beam subjected to fire (see Figure 10a), the experimental data from the unstrengthened specimen (RC) [32] were assigned for comparative purposes. The comparison of the displacement-temperature curves of the simply supported RC beam and CFRP-strengthened beams from the experimental tests and FEA are presented in Figure 10a and Figure 10b, respectively. The results are presented in terms of ultimate failure for the RC beam and strengthening debonding for CFRP-strengthened beam. The mechanical results developed after the strengthening system debonding (ultimate failure of the strengthened beam) is not presented, since it is not relevant to bond analysis.
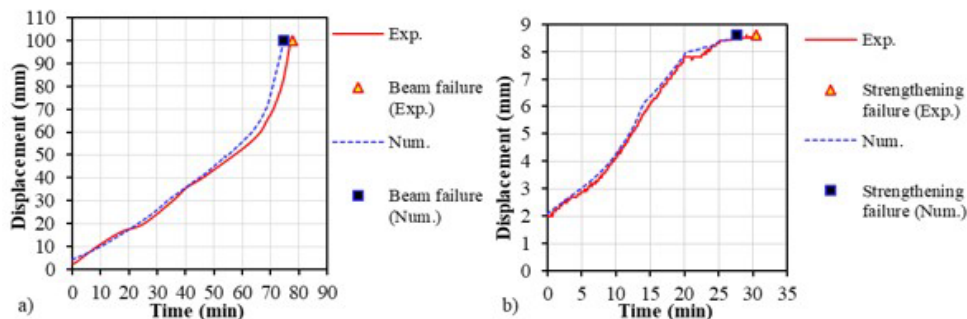

Figure 10. Experimental (Exp.) [32] and predicted (Num.) displacement-temperature curves for the a) unstrengthened and b) CFRP-strengthened RC beams, in terms of ultimate beam failure and strengthening system debonding, respectively

Similar tendencies with an equivalent slope were obtained from the FEA in comparison with the experimental results [32] for both RC beam and CFRP-strengthening system (specimens RC and EC-35, respectively). The experimental curves presented a slightly higher stiffness than the numerical ones, indicating that the respective predicted data is on the safe side. A good agreement between the FEA and experimental [32] analysis in terms of critical fire resistance time for the RC beam (FR_{time}) was obtained, as shown in Table 1. The failure instant of this beam was experimentally achieved at 78.2 min of fire exposure, while for the numerical model a fit close and slight conservative time of 74.5 min was noticed. In the case of strengthened beam, a satisfactory convergence of results between the models was also obtained. The fire resistance time at the CFRP debonding instant ($FR_{time,CFRP}$) for the strengthened beam was quite similar for both experimental and numerical models, corresponding to 30.5 and 27.7 min, respectively, as shown in Table 1. Therefore, the results showed that the differences between experimental and numerical fire resistance times were less than 5% and 10%, respectively for unstrengthened RC beam and CFRP-strengthening system (Table 1). In addition, a relationship between the FR_{time} or $FR_{time,CFRP}$ at different displacements obtained by the numerical and experimental analysis for both types of beams was also presented in Table 1.

Table 1. Experimental (Exp.) [32] and numerical (Num.) fire resistance time at different displacements of unstrengthened beam and CFRP-strengthening system.

unstrengthened RC beam	FR_{time} at 50 mm displacement (min)		FR_{time} at 75 mm displacement (min)		FR_{time} at beam failure instant (min)		FR_{time} ratio at failure instant of the beam
	Exp. [32]	Num.	Exp. [32]	Num.	Exp. [32]	Num.	
	57.0	54.9	72.3	69.5	78.2	74.5	0.95
CFRP-strengthening system	$FR_{time,CFRP}$ at 5 mm displacement (min)		$FR_{time,CFRP}$ at 8 mm displacement (min)		$FR_{time,CFRP}$ at CFRP failure instant (min)		$FR_{time,CFRP}$ ratio at failure instant of the CFRP system
	Exp. [32]	Num.	Exp. [32]	Num.	Exp. [32]	Num.	
	12.2	11.8	23.0	20.1	30.5	27.7	0.91

Notwithstanding the slight differences above mentioned, the models presented general good agreement and accuracy between the experimental and numerical results of the RC beam and CFRP-strengthening system. All these

Rev. IBRACON Estrut. Mater., vol. 16, no. 2, e16202, 2023

12/18

results indicate that the estimated data is generally on the safe side but not too conservative, though. The satisfactory agreement and accuracy between the experimental and numerical results confirm the validity of the developed FE models and attest to their ability to simulate the mechanical response of simply supported RC and CFRP-strengthened beams under fire conditions.

5.3 Failure mode analysis

The numerical failure modes of the tested specimens under four-point bending configuration and at ambient temperature conditions obtained from the FEA are illustrated in Figure 11a to Figure 15a and they are compared to the experimental failure modes as shown in Figure 11b and Figure 15b.

The bending failure mode characterized by excessive deflections and flexural cracks at mid-span, without lateral displacements, due to tensile rupture and excessive elongation of the bottom rebars that were responsible for the collapse of the experimentally tested unstrengthened RC beams were also clearly identified in the predicted failure modes. Figure 11 shows a view of (a) numerical and (b) experimental deformed shape of the RC beam at the failure instant. Moreover, the cracking along the cross-section of the beam was also registered and a good similarity was achieved between the numerical and experimental models, as shown in Figure 12a and Figure 12b, respectively.
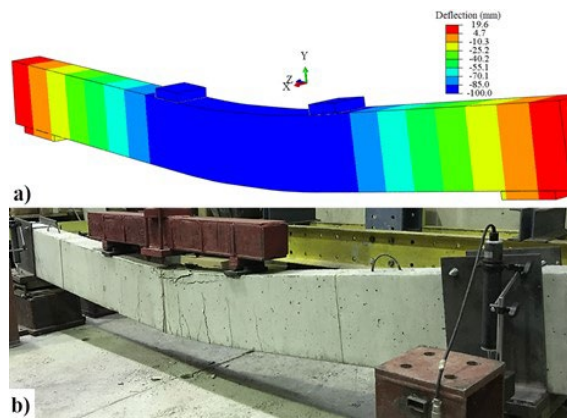

Figure 11. (a) Numerical (b) and experimental deformed shape for the unstrengthened RC beam (specimen RC_AT) at the failure instant: view 1
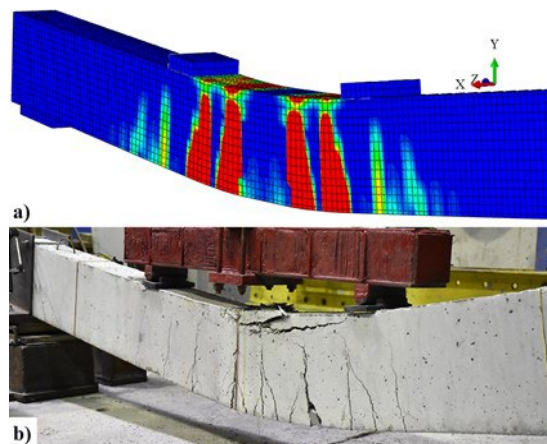

Figure 12. (a) Numerical (b) and experimental cracking along the cross-section of the unstrengthened RC beam (specimen RC_AT) at the failure instant: perspective view

Regarding the failure modes of the CFRP-strengthened beam at ambient temperature, that was characterized by the debonding of strengthening system in the CFRP-concrete bond region, a good agreement between the numerical and the experimental failure modes was noticed, as shown in Figure 13a and Figure 13b, respectively.
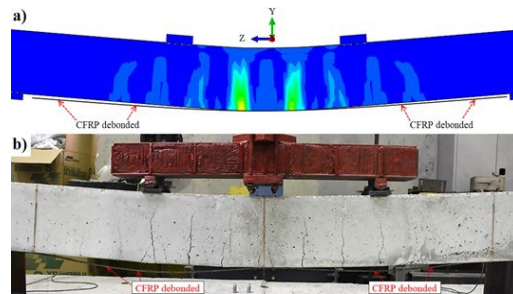

Figure 13. (a) Numerical (b) and experimental failure modes for the CFRP-strengthened RC beam (specimen CFRP_AT) after the laminate collapse

The debonding of the CFRP system was assumed when a displacement peak was observed in the strengthened beam while an excessive and abrupt unloading of the system occurred.

Furthermore, the deformed shape of the strengthened beam at the CFRP failure instant was precisely predicted by the FE model, as noticed in Figure 14. Similarities regarding the cracking along the cross-section of the strengthened specimen were also numerically estimated successfully as shown in Figure 15.
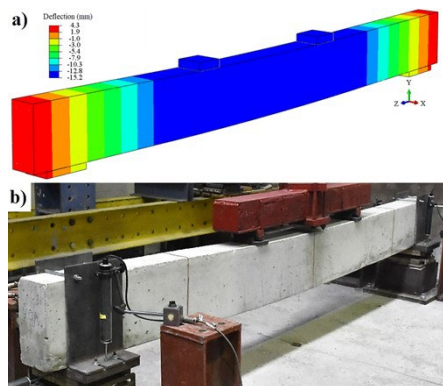

Figure 14. (a) Numerical (b) and experimental deformed shape for the CFRP-strengthened beam (specimen CFRP_AT)) at the CFRP failure instant
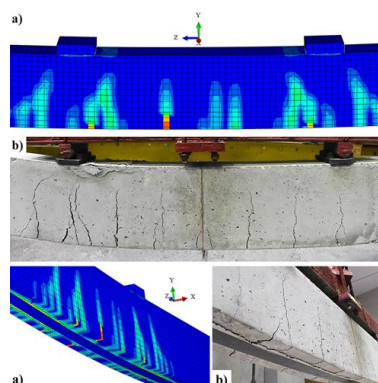

Figure 15. (a) Numerical (b) and experimental cracking along the cross-section of the CFRP-strengthened beam at the CFRP failure instant

The results above confirm that the finite element models predicted the failure modes of unstrengthened and CFRP-strengthened beams with good precision, attesting their consistency to simulate the mechanical response of this type of structures at ambient temperature. Furthermore, the mechanical validation of the model at ambient temperature allowed the FE model to assess mechanical analyses under fire conditions (Section 5.2).

5.4 Heat transfer analysis

The suitability of 2D thermal models developed using the heat transfer option available in Abaqus was assessed in this section. The purpose of this numerical approach was to determine the appropriate modelling parameters especially the input thermal boundary conditions and material thermal properties, so that standard fire resistances tests of unstrengthened and CFRP-strengthened RC beams can be simulated. It should be also noted that a uniform temperature along the entire longitudinal length of the beam was intended for the validation study, in contrast to the recorded at the mid-spam cross-section of beams tested in Laboratory [32]. Moreover, to calibrate the FE model for fire simulation of CFRP-strengthened RC beams, the furnace fire curve data registered from the fire resistance tests [32] were used. Note that the emissivity, the heat transfers, and the thermal contact conductance coefficients were constant with temperature evolution. The radiative heat flux was calculated as 0.49 using an emissivity of 0.7 for fire and 0.7 for the concrete surface. The Stefan-Boltzmann constant was defined as 5.67×10^{-8} W/m^{2}K^4. Figure 16b, Figure 16c and Figure 16d shows respectively the comparison between experimental (Exp.) [32] and predicted (Num.) temperatures as a function of fire exposure time for the different thermocouples at mid-span of the CFRP-strengthened beams fire-protected. The CFRP-strengthened RC beams were protected by three types of fire protection systems composed by VP, EC, and OP cement-based mortars. Moreover, a 35 mm thickness on the fire protection system was adopted. The specimens were referred to as EC-35, OP-35 and VP-35 for VP, EC and OP mortars fire protected with 35 mm thick, respectively.

The temperature vs. fire exposure time evolution for the different thermocouples of the unstrengthened and unprotected RC beam (referred as RC) is shown in Figure 16a. It is worthwhile mentioning that the temperature evolution in the CFRP-strengthened RC beams was presented in Figure 16bcd only until the collapse instant of the respective fire protection material reported in the experimental data [32], since the results after that time are negligible for the purpose of this numerical study. Regarding the RC beam, the results were plotted in Figure 16a until the collapse of the beam.
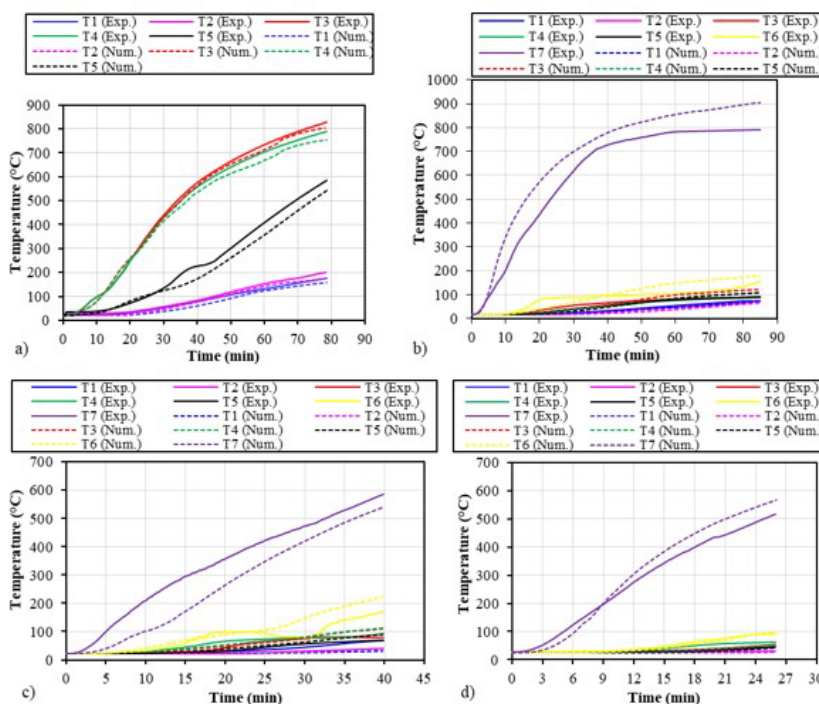

Figure 16. Experimental (Exp.) [32] and predicted (Num.) temperatures vs. fire exposure time curves at different points of the mid-span cross-section for the beams: a) RC, b) VP-35, c) OP-35 and d) EC-35

Overall, all FE models provided a good agreement with the experimental results in terms of temperature evolution, as noticed in the Figure 16a-d. With exception of thermocouples T6 and T7 (positioned on the bottom surfaces of the laminate and the fire protection material, respectively) for the strengthened beams protected by OP and VP mortar, all other temperature distributions at different points of the cross-section were accurately predicted by the models. Small deviations between Exp. and Num. temperatures in T6 and T7 of the VP-35 and OP-35 beams were observed, as depicted in Figure 16b and Figure 16c, respectively. Despite that, the FE models were still able to simulate the thermal behavior tendency with a relative consistency in the above-mentioned thermocouples. Concerning the strengthened EC-35 and RC beams (Figure 16a and Figure 16d, respectively), the numerical results by the heat transfer analysis presented an excellent convergence with the experimental measurements for all thermocouples. To sum up, the tools of Abaqus program for the application of thermal actions allowed simulating the phenomenon of heat transfer between hot air and composite structural elements with satisfactory results. Despite the above-mentioned deviations, all models overall provided a good estimate between the experimental and numerical results, confirming the ability of the FE models to accurately simulate the thermal response of unstrengthened and EBR-CFRP-strengthened RC beams subjected to fire, even when using complex and different fire protection materials.

6 CONCLUSIONS

The structural behavior of RC beams flexurally strengthened with CFRP laminates bonded according to the EBR technique and unstrengthened RC beams was numerically investigated in this paper. Finite element models capable of simulating the mechanical and thermal response of simply supported unstrengthened and CFRP-strengthened RC beams both under ambient and fire conditions were developed and described in the current research. Numerical simulations using the finite element software Abaqus has been performed. The results obtained from the numerical study presented herein allow to draw the following conclusions:

- The thermal response of the fire-protected CFRP-strengthened RC beams subjected to high temperatures was accurately predicted by the FE models, similarly to the heat transfer analysis of the unprotected and unstrengthened RC beam. Moreover, the modelling of the surrounding building slab allowed it to represent the thermal interactions and influence between the elements as faithful as possible, providing a better predicting of the experimental results and, consequently, more realistic.
- Concerning the prediction of the mechanical response at ambient temperature, the 3D models presented a satisfactory accuracy for both unstrengthened and CFRP-strengthened RC beams, especially for estimating the ultimate load capacity.
- The developed finite element models also estimate with precision the mechanical response of unstrengthened and CFRP-strengthened RC beams simultaneously subjected to a flexural load and high temperatures. An accuracy of about 91% and 95% was respectively achieved by the numerical models that represent the RC and CFRP-strengthened RC beams, compared to the experimental results in terms of failure instant.
- The failure modes of the beams and the aspects after the test were also estimated with accuracy by the finite element models. The predictions of deformed shape, failure and cracking aspects, stresses on the steel reinforcements and, especially, the CFRP failure aspect in the strengthened beams, were very similar to the ones observed in the reference experimental models tested.
- Finally, the presented results confirmed the validity of the developed FE models and strongly guaranteed an accurate prediction of the mechanical response of both strengthened and unstrengthened RC beams at ambient and high temperatures. Furthermore, it is still possible to stated that this developed FE models can be used as a valuable auxiliary tool for the design of fire protection systems for CFRP-strengthened RC structural members or in parametric studies outside the bounds of experimental field, as well as provide safe and economical structural solutions for these type of structures in fire situations.

REFERENCES

[1] M. Mohammadi, M. Barghian, D. Mostofinejad, and A. Rafieyan, "Alkali and temperature long-term effect on the bond strength of fiber reinforced polymer-to-concrete interface," *J. Compos. Mater.*, vol. 52, no. 15, pp. 2103–2114, Jun. 2018, http://dx.doi.org/10.1177/0021998317740201.

[2] N. Dodds, A. G. Gibson, D. Dewhurst, and J. M. Davies, "Fire behaviour of composite laminates," *Compos., Part A Appl. Sci. Manuf.*, vol. 31, no. 7, pp. 689–702, Jul. 2000, http://dx.doi.org/10.1016/S1359-835X(00)00015-4.

[3] A. P. Mouritz and A. G. Gibson, *Fire Properties of Polymer Composite Materials.* Dordrecht: Springer, 2006.

[4] A. J. B. Tadeu and F. J. F. G. Branco, "Shear tests of steel plates epoxy-bonded to concrete under temperature," *J. Mater. Civ. Eng.*, vol. 12, no. 1, pp. 74–80, Feb. 2000, http://dx.doi.org/10.1061/(ASCE)0899-1561(2000)12:1(74).

[5] American Concrete Institute, *Guide for the Design and Construction of Externally Bonded FRP Systems for Strengthening Existing Structures*, ACI 440.2R-17, 2017.

[6] R. A. Hawileh, M. Naser, W. Zaidan, and H. A. Rasheed, "Modeling of insulated CFRP-strengthened reinforced concrete T-beam exposed to fire," *Eng. Struct.*, vol. 31, no. 12, pp. 3072–3079, 2009, http://dx.doi.org/10.1016/j.engstruct.2009.08.008.

[7] A. Ahmed and V. K. R. Kodur, "Effect of bond degradation on fire resistance of FRP-strengthened reinforced concrete beams," *Compos., Part B Eng.*, vol. 42, no. 2, pp. 226–237, Mar. 2011, http://dx.doi.org/10.1016/j.compositesb.2010.11.004.

[8] J. G. Dai, W. Y. Gao, and J. G. Teng, "Finite element modeling of insulated FRP-strengthened RC beams exposed to fire," *J. Compos. Constr.*, vol. 19, no. 2, 2010, http://dx.doi.org/10.1061/(ASCE)CC.1943-5614.0000509.

[9] J. P. Firmo, M. R. T. Arruda, and J. R. Correia, "Numerical simulation of the fire behaviour of thermally insulated reinforced concrete beams strengthened with EBR-CFRP strips," *Compos. Struct.*, vol. 126, pp. 360–370, 2015, http://dx.doi.org/10.1016/j.compstruct.2015.02.084.

[10] J. P. Firmo, M. R. T. Arruda, J. R. Correia, and I. C. Rosa, "Three-dimensional finite element modelling of the fire behaviour of insulated RC beams strengthened with EBR and NSM CFRP strips," *Compos. Struct.*, vol. 183, no. 1, pp. 124–136, 2018, http://dx.doi.org/10.1016/j.compstruct.2017.01.082.

[11] B. Williams, V. Kodur, M. F. Green, and L. Bisby, "Fire endurance of fiber-reinforced polymer strengthened concrete T-Beams," *ACI Struct. J.*, vol. 105, no. 1, pp. 60–67, 2008.

[12] ANSYS, *Finite Element Computer Code, Version 11.* Canonsburg, USA: ANSYS Inc., 2007.

[13] American Society for Testing and Materials, *Standard Test Methods for Fire Tests of Building Construction and Materials*, ASTM E119, 2002.

[14] V. K. R. Kodur and A. Ahmed, "Numerical model for tracing the response of FRP-strengthened RC beams exposed to fire," *J. Compos. Constr.*, vol. 14, no. 6, pp. 730–742, Dec. 2010, http://dx.doi.org/10.1061/(ASCE)CC.1943-5614.0000129.

[15] H. Blontrock, L. Taerwe, and P. Vandevelde, "Fire tests on concrete beams strengthened with fibre composite laminates," in *Proceedings of the third Ph.D. symposium,* K. Bergmeister, Eds. Vienna*, 2000, pp. 151–161. Accessed: Mar. 29, 2022. [Online]. Available: http://hdl.handle.net/1854/LU-130382

[16] A. Ahmed and V. Kodur, "The experimental behavior of FRP-strengthened RC beams subjected to design fire exposure," *Eng. Struct.*, vol. 33, no. 7, pp. 2201–2211, 2011, http://dx.doi.org/10.1016/j.engstruct.2011.03.010.

[17] H. V. S. GangaRao, N. Taly, and P. V. Vijay, *Reinforced concrete design with FRP composites.* Boca Raton, USA: CRC Press, 2007.

[18] ABAQUS, *Analisys Standard User's Manual, Version 6.8.* Rhode Island, USA: Dassault Systèmes, 2008.

[19] International Federation for Structural Concrete, *The FIB Model Code for Concrete Structures: Model Code.* Lausanne: FIB, 1990.

[20] J. P. Firmo and J. R. Correia, "Fire behaviour of thermally insulated RC beams strengthened with EBR-CFRP strips: Experimental study," *Compos. Struct.*, vol. 122, pp. 144–154, Apr. 2015, http://dx.doi.org/10.1016/j.compstruct.2014.11.063.

[21] J. P. Firmo, M. R. T. Arruda, and J. R. Correia, "Contribution to the understanding of the mechanical behaviour of CFRP-strengthened RC beams subjected to fire: Experimental and numerical assessment," *Compos., Part B Eng.*, vol. 66, pp. 15–24, 2014, http://dx.doi.org/10.1016/j.compositesb.2014.04.007.

[22] ABAQUS, *Analisys Standard User's Manual, Version 6.11.* Rhode Island, USA: Dassault systèmes, 2011.

[23] E. Klamer, "Influence of temperature on concrete beams strengthened in flexure with CFRP," Ph.D. dissertation, Eindhoven University of Technology, Eindhoven, 2009. [Online]. Available: http://dx.doi.org/10.6100/IR656177.

[24] J. Dai, W. Y. Gao, and J. G. Teng, "Bond-slip model for FRP laminates externally bonded to concrete at elevated temperature," *J. Compos. Constr.*, vol. 17, no. 2, pp. 217–228, Apr. 2013, http://dx.doi.org/10.1061/(ASCE)CC.1943-5614.0000337.

[25] J. Dai, T. Ueda, and Y. Sato, "Development of the nonlinear bond stress–slip model of fiber reinforced plastics sheet–concrete interfaces with a simple method," *J. Compos. Constr.*, vol. 9, no. 1, pp. 52–62, 2005, http://dx.doi.org/10.1061/(ASCE)1090-0268(2005)9:1(52).

[26] W. Y. Gao, J. G. Teng, and J. Dai, "Effect of temperature variation on the full-range behavior of FRP-to-concrete bonded joints," *J. Compos. Constr.*, vol. 16, no. 6, pp. 671–683, Dec. 2012, http://dx.doi.org/10.1061/(ASCE)CC.1943-5614.0000296.

[27] J. C. P. H. Gamage, R. Al-Mahaidi, and M. B. Wong, "Bond characteristics of CFRP plated concrete members under elevated temperatures," *Compos. Struct.*, vol. 75, no. 1–4, pp. 199–205, 2006, http://dx.doi.org/10.1016/j.compstruct.2006.04.068.

[28] M. R. T. Arruda, J. P. Firmo, J. R. Correia, and C. Tiago, "Numerical Modelling of the bond between concrete and CFRP laminates at elevaded temperatures," *Eng. Struct.*, vol. 110, pp. 233–243, Mar. 2016, http://dx.doi.org/10.1016/j.engstruct.2015.11.036.

[29] European Committee for Standardization, *Eurocode 2: Design of Concrete Structures - Part 1-1 : General Rules and Rules for Buildings*, EN 1992-1-1, 2004.

[30] European Committee for Standardization, *Eurocode 2: Design of Concrete Structures - Part 1-2: General rules - Structural Fire Design*, EN 1992-1-2, 2004.

[31] International Federation for Structural Concrete, *FIB Bulletin 14: Externally Bonded FRP Reinforcement for RC Structures.* Lausanne: FIB, 2001.

[32] T. B. Carlos, J. P. C. Rodrigues, R. C. A. Lima, and D. Dhima, "Experimental analysis on flexural behaviour of RC beams strengthened with CFRP laminates and under fire conditions," *Composite Structures*, vol. 189, no. 2017, pp. 516–528, 2018, http://dx.doi.org/10.1016/j.compstruct.2018.01.094.

[33] T. B. Carlos and J. P. C. Rodrigues, "Experimental bond behaviour of a CFRP strengthening system for concrete elements at elevated temperatures," *Constr. Build. Mater.*, vol. 193, pp. 395–404, Dec. 2018, http://dx.doi.org/10.1016/j.conbuildmat.2018.10.184.

[34] ABAQUS CAE, *Abaqus Analisys User's Guide, Version 6.14*. Rhode Island, USA: Dassault systèmes, 2015.

[35] L. Laím, J. Paulo, C. Rodrigues, and L. Simões, "Experimental and numerical analysis on the structural behaviour of cold-formed steel beams," Ph.D. dissertation, University of Coimbra, Coimbra, Portugal, 2013.

[36] ABAQUS CAE, *Abaqus Theory Guide, Version 6.14*. Rhode Island, USA: Dassault Systèmes, 2015.

[37] Association Française de Normalisation, *Eurocode 2: Calcul des Structures en Béton - Partie 1-2: Règles Générales - Calcul du Comportement au Feu*, NF EN 1992-1-2 (Annexe Nationale), 2007.

[38] European Committee for Standardization, *Eurocode 4: Design of Composite Steel and Concrete Structures - Part 1-2: General Rules - Structural Fire Design,* EN 1994-1-2, 2005.

[39] C. A. Griffis, R. A. Masumura, and C. I. Chang, "Thermal response of graphite epoxy composite subjected to rapid heating," *J. Compos. Mater.*, vol. 15, no. 5, pp. 427–442, Sep. 1981., http://dx.doi.org/10.1177/002199838101500503.

[40] J. P. Firmo, J. R. Correia, and P. França, "Fire behaviour of reinforced concrete beams strengthened with CFRP laminates: Protection systems with insulation of the anchorage zones," *Compos., Part B Eng.*, vol. 43, no. 3, pp. 1545–1556, 2012, http://dx.doi.org/10.1016/j.compositesb.2011.09.002.

[41] Simpson Strong-Tie Company, "S&P C-Laminate: Carbon fiber polymer plates for structural reinforcement: product technical specifications." S&P. http://www.sp-reinforcement.eu/sites/default/files/field_product_col_doc_file/suiss_c-laminates_e_ver022018_co-branded_0.pdf (accessed Mar. 29, 2018).

[42] Perlita y Vermiculita, *Biofire: Product Technical Specifications*. Barcelona: Perlita y Vermiculita, 2008.

[43] Secil Martingança, *RHP Manual Interior: Product Technical Specifications*. Leiria: Secil Martingança, 2013.

[44] S. A. Argex, *ARGEX® 0-2: Product Technical Information*. Aveiro: Argex, 2008.

[45] K. Wang, B. Young, and S. T. Smith, "Mechanical properties of pultruded carbon fibre-reinforced polymer (CFRP) plates at elevated temperatures," *Eng. Struct.*, vol. 33, no. 7, pp. 2154–2161, 2011, http://dx.doi.org/10.1016/j.engstruct.2011.03.006.

[46] L. A. Bisby, *Fire Behaviour of FRP Reinforced or Confined Concrete.* Kingston: Queen's University, 2003.

[47] Ø. T. Moltubakk, "Nonlinear analysis of fibre reinforced concrete beams: Influence of fibre orientation and density," M.S. thesis. Norwegian University of Science and Technology, Trondheim, 2014. [Online]. Available: https://docplayer.net/62653923-Nonlinear-analysis-of-fibre-reinforced-concrete-beams.html

[48] J. A. O. Barros, *Modelos de Fendilhação para o Betão*. Porto: Universidade do Minho, 1996.

Rev. IBRACON Estrut. Mater., vol. 16, no. 2, e16202, 2023

18/18